Resynchronization of Islanded Virtual Synchronous Machines by Cascaded Phase and Frequency Controllers Acting on the Internal Power Reference

[*]Francesco Giudicepietro, [†]Salvatore D'Arco, [†,#]Jon Are Suul, [*]Luigi Piegari

[*]Department of Electronics, Information and Bioengineering, Politecnico di Milano. Milano, Italy

[†]SINTEF Energy Research, Trondheim, Norway

[#]Department of Engineering Cybernetics, Norwegian University of Science and Technology, Trondheim, Norway

e-mail: francesco.giudicepietro@mail.polimi.it, salvatore.darco@sintef.no, Jon.A.Suul@sintef.no, luigi.piegari@polimi.it

***Abstract*—Virtual Synchronous Machines (VSMs) have the capability to operate in grid connected or in islanded mode in the same way as synchronous machines. Furthermore, VSMs can inherently support seamless transition from grid connected to islanded mode. However, the reconnection of a VSM-based islanded to the grid requires a dedicated synchronization controller. The synchronization process should align the frequency and phase angle of the islanded system to the grid voltage to avoid abrupt transients in the currents when closing the breaker connection to the grid. This paper presents a simple and flexible control structure for grid resynchronization of a VSM operating in islanded mode. The scheme is based on two cascaded regulators operating on the phase and frequency difference between the VSM and the grid to generate an offset in the power reference. Starting from a simplified analytical model of the islanded system, a tuning procedure ensuring a controlled resynchronization transient is derived. Numerical results confirm the intended operation of the synchronization scheme with the associated tuning algorithm and validate their robustness against variations in the initial conditions of the synchronization process and to the virtual inertia value.**

Keywords— Islanded power systems, Frequency Control, Phase Control, Power Control, Virtual Synchronous Machines

I. INTRODUCTION

Control strategies for operating power electronic converters as virtual synchronous machines (VSM) have been widely studied during the last decade [1]-[4]. Such control strategies are designed to emulate the inertial dynamics and power-balance-based synchronization mechanism of synchronous machines (SMs). Thus, VSM-controlled converters can provide virtual inertia in power systems with declining share of traditional SM-based generation. Furthermore, VSMs have the same operational flexibility as SMs in terms of ability to operate in both grid connected and islanded modes. Therefore, VSM-based control can be suitable for microgrids and other applications that require converters with grid forming capability [5]-[7].

Due to the grid forming capability of VSMs, the transition between grid connected and islanded mode is in general seamless and require no changes in the control. However, the opposite transition requires a synchronization process in a similar way as necessary for SM-based power plants or SM-based microgrids [8]-[10]. Indeed, the reconnection of two asynchronous parts of a power system requires the differences in phase and frequency to be eliminated before closing the breaker between them, to avoid over-currents and severe transients.

Several recent publications have proposed methods for re-synchronization of islanded microgrids when they should be reconnected to the main grid [9]-[15]. The developed control methods are then intended to eliminate the frequency and phase angle differences between the islanded grid and the main grid, so that the breaker separating them can be closed without causing any significant transient. Although this can be achieved by adding dedicated converters for enforcing alignment between the islanded grid and the main grid [15], such methods can add significant cost. Thus, solutions with a centralized resynchronization controller providing references to the individual generation units is usually preferred for reconnection of islanded systems to the main grid, for converter-based systems as well as systems containing conventional generation units[10], [11].

Since the VSM concept itself is intended for explicitly emulating the dynamics of SMs, one natural approach for designing control strategies for reconnection to the main grid is to utilize similar synchronization strategies as developed for grid connection of synchronous generators. This implies that the resynchronization controller is designed to act on the frequency reference for the VSM [11], [12]. However, utilization of the frequency reference can lead to a conflict between the control for eliminating the phase and frequency deviations from the main grid. In [11], this was solved by introducing a parallel structure for controlling the frequency and phase deviations, and the phase angle control was disabled when the frequency deviation was large. Similarly, a parallel structure where the phase angle deviation is corrected by actively offsetting the phase angle generated within the virtual swing equation of the VSM was proposed in [13], [14]. However, such approaches add complexity and complicates the tuning of the synchronization controller.

This paper presents a scheme for synchronization of a VSM to the grid based on a cascaded control with two regulators controlling an offset in the power reference. The inner loop aims at synchronizing the frequency while the outer loop aligns the phase of the voltage on the two sides of the breaker separating the islanded system from the main grid. The concept is adapted from a converter-based strategy for synchronization of SMs as proposed in [16]. By utilizing a simplified model for the islanded operation of a VSM, a

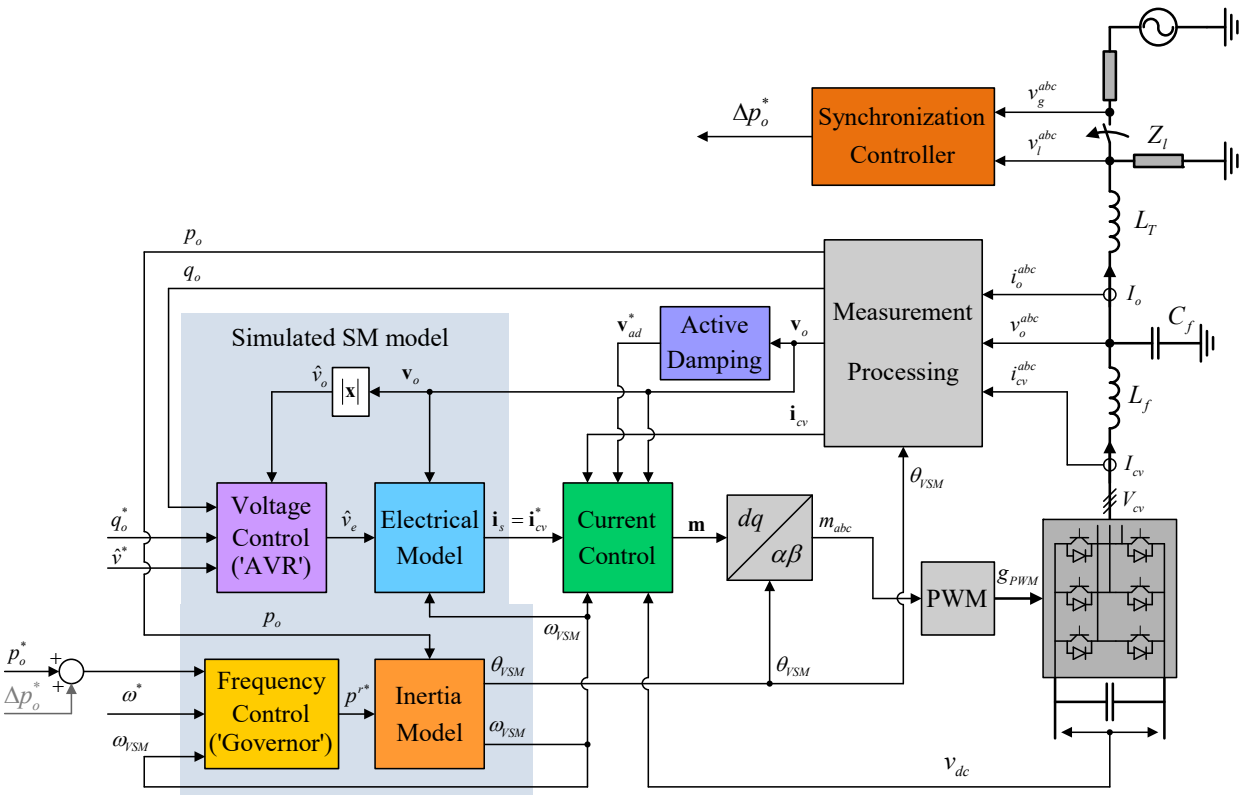

Fig. 1 Overview of control structure for Current Controlled Virtual Synchronous Machine with outer loop control for resynchronization to an external grid

tuning procedure for the proposed control scheme is also derived. The proposed tuning provides a simple way of selecting the parameters for the proposed controller while shaping the transient response. The performance of the synchronization controller and the associated tuning procedure have been validated by numerical simulations. The results confirm that the synchronization process is executed according to the design specifications and that it is robust with respect to the parameters of the VSM and the initial conditions when the synchronization procedure is started.

II. Studied System Configuration

As a basis for developing the proposed synchronization controller, a simple system configuration including an example of a VSM-based control scheme is utilized.

A. System configuration

The reference configuration for assessing the synchronization process is illustrated in Fig. 1. In this figure and all following discussions, upper case symbols represent physical signals and parameters, while lower case symbols represent per unit quantities. A converter controlled as a VSM is connected to a local load represented as a constant impedance. The converter and the load can be connected to an external grid with a controllable breaker. Thus, the converter and load can be operated in grid connected mode or in islanded mode where the VSM is entirely responsible for the voltage and frequency regulation of the local grid. The voltages at both sides of the breaker are measured and used as input to the proposed synchronization controller

B. Virtual Synchronous Machine Implementation

The proposed synchronization scheme is intended to be applicable for any VSM-based control strategy relying on an emulated swing equation [2]. As an example, a current

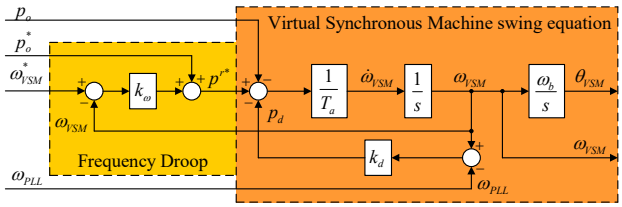

Fig. 2 Virtual swing equation of the VSM with frequency droop on the power input

controlled VSM (CCVSM) implemented according to [17] is utilized as a reference control structure, as shown in Fig. 1. At the core of the VSM implementation is a virtual swing equation representing the inertial dynamics of an emulated SM. The emulated inertia model, including a frequency droop in the input power, can be illustrated by a block diagram as shown in Fig. 2 and expressed as dynamic equation given by:

$$T_a \frac{d\omega_{VSM}}{dt} = p^* + k_\omega\left(\omega^*_{VSM} - \omega_{VSM}\right) - p_o + k_d\left(\omega_{VSM} - \omega_{PLL}\right) \quad (1)$$

In this equation ω_{VSM} is the emulated speed of the virtual inertia, T_a (=2H) is the inertia time constant, k_ω is the frequency droop coefficient, k_d is the damping coefficient and p_o is the electrical power output from the converter. The external inputs to the model include a power reference p_o^* and a frequency reference ω^*_{VSM}. The main adaptation compared to the implementation in [17] is that the internal damping of the inertial dynamics is calculated from the difference between the VSM speed and the external frequency ω_{PLL} as measured from a PLL, according to [18]. A block diagram of the applied PLL structure is reported in Fig. 3, adapted from [19], [20].

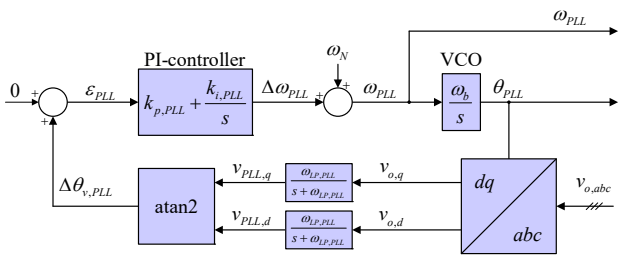

Fig. 3 Schematic of the PLL control structure

TABLE I
PARAMETERS OF THE INVESTIGATED CONFIGURATION

Parameter	Value	Parameter	Value]
AC Voltage $V_{g,n}$	690 V	Rated current	2300 A
Rated angular frequency ω_n	2π·50 rad/s	Primary filter inductance l_f r_{lf}	0.08pu, 0.005pu
Filter capacitance c_f	0.08 pu	Grid-side filter inductance l_l r_{Ll}	0.05pu, 0.005pu
dc voltage V_{dcn}	1200 V	Active damping TfAD, k_AD	50 ms 1.0 pu
Current controller gains, kpc,kic	12.73 2500	PLL filter, $T_{f,PLL}$	2 ms
CC VSM QSEM Impedance, r_v, l_v	0.04 pu 0.25 pu	PLL PI controller, kpPLL, kiPLL	0.0844 4.69
Virtual inertia T_a	2 s	VSM damping kd	40 pu
Frequency droop k_ω	20 pu	Reactive power droop k_q	0.05 pu
Reactive power measurement filter	100 rad/s	Voltage measurement filter	10 rad/s

The inner current loop for the CCVSM in Fig. 1 is a conventional current control in the Synchronously Rotating Reference Frame (SRRF) aligned with the VSM position. The current references are generated from a quasi-stationary electrical model (QSEM) represented by a virtual impedance according to:

$$\mathbf{i}_s = \frac{\hat{v}_e - \mathbf{v}_{o,m}}{r_v + j\omega_{VSM} l_v} \tag{2}$$

where r_v and l_v are the virtual resistance and virtual inductance, and $\hat{v}_e$ is the reference voltage amplitude. The variable $\boldsymbol{v}_{o,m}$ represents a filtered version of the output voltage $\boldsymbol{v}_o$ measured at the filter capacitors, where the filtering is provided by first order low pass filters acting on the *d*- and *q*-axis components individually. The result from (2) is the virtual stator current of the VSM, $\mathbf{i}_s$, which is used as the current reference $\mathbf{i}_{cv}^*$ for the control of the converter.

C. Study Case Parameters

In the following sections the proposed synchronization controller will be designed and analysed on basis of the configuration from Fig. 1. For this purpose, the parameters reported in the Table I will be utilized to generate all numerical results.

III. SYNCHRONIZATION CONTROLLER DESIGN

The basic structure and general functionality of the proposed synchronization controller is introduced in the following. The general controller structure is then combined with a simplified model of system configuration from Fig. 1 as a basis for deriving a proposed tuning procedure.

A. Proposed Synchronization Controller

The proposed synchronization controller aims at aligning the frequency and phase angle of the voltage in the islanded

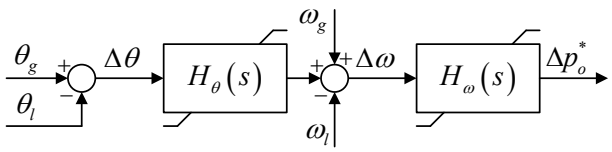

Fig. 4 Proposed control loop for providing the synchronizing power reference to the VSM

system with the grid voltage at the connection point. Instead of designing the synchronization controller to modify the frequency reference for the VSM as the methods in [11], [12], the proposed synchronization controller is instead actively offsetting the power reference input to the emulated swing equation. This approach is adapted from the strategy for converter-assisted synchronization of SMs proposed by [16], and it will be shown that this allows for a simple and robust synchronization structure without the need for additional weighting mechanisms as required for the parallel structure applied in [11].

A schematic diagram of the synchronization controller is reported in Fig. 4. The structure consists of two cascaded regulators. The inner control loop is operating with an input given by the frequency difference between the grid and the islanded system, summed with the output of the outer loop regulator. The output of this regulator is saturated and added to the external power reference for the VSM. This loop ensures an alignment of the frequency of the virtual inertia with the external grid at steady state. The alignment of the phase is obtained from an outer loop proportional regulator acting on the phase error.

The overall synchronization controller indicated in Fig. 1 consists of the control loops in Fig. 4 and two PLLs operating on the voltage measurements at each side of the breaker for providing the phase and frequency input signals to the controller. When the phase and frequency differences across the breaker are sufficiently close to zero, the synchronization process can be assumed completed and the VSM can be reconnected to the grid. The general requirements for the controller can be expressed in terms of reducing the time for achieving the synchronization while ensuring a smooth transient without oscillations.

B. Simplified system modelling

The VSM operates based on a virtual swing equation that links the transient behaviour of the internal virtual speed ω_{VSM} with the power and frequency reference. Assuming relatively slow variations in the VSM speed so that the effect of the internal damping can be ignored, the small signal transfer function between the power reference and the frequency of the islanded system can be derived from:

$$\frac{\Delta p_o^* - k_\omega \Delta\omega_{VSM}}{T_a}\frac{1}{s} = \Delta\omega_{VSM} \tag{3}$$

where the symbol Δ indicates small signal increments of the associated variable and *s* is the Laplace operator. Thus, the transfer function linking the power reference to the emulated speed of the virtual inertia can be expressed as:

$$\Delta\omega_{VSM} = \frac{\Delta p_o^*}{T_a s + k_\omega} \tag{4}$$

The expression in (4) clearly indicates the direct functional relation between the power reference and the virtual speed as a first order transfer function for the time scale of interest.

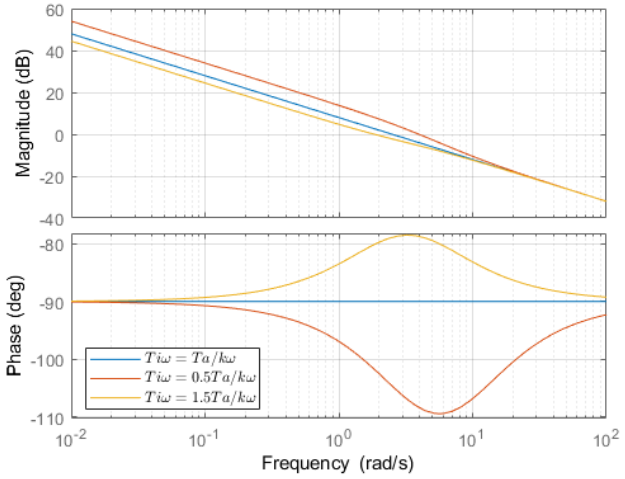

Fig. 5. Bode diagram of the open loop transfer function of the frequency controller

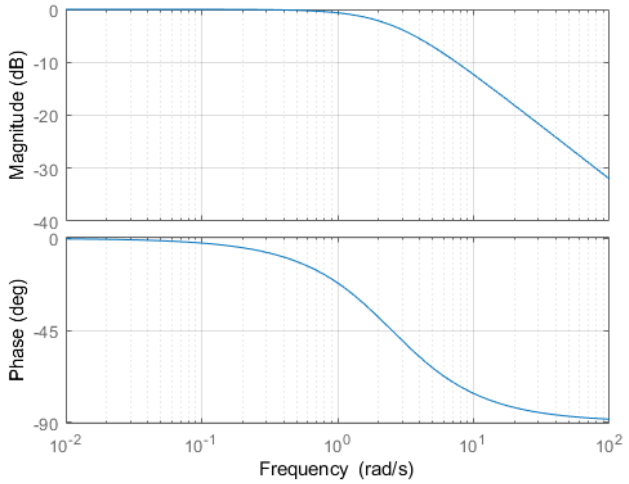

Fig. 6. Bode diagram of the closed loop transfer function for frequency controller

C. *Design of Inner Frequency Control Loop*

Assuming that the inner loop controller should be based on a PI regulator, the open loop transfer function can be expressed as:

$$H_{OL\omega}(s) = k_{p\omega}\frac{1+T_{i\omega}s}{T_{i\omega}s}\frac{1}{T_a s + k_\omega} \tag{5}$$

where $k_{p\omega}$ is the proportional gain and $T_{i\omega}$ is the integral time constant of the regulator.

Given the characteristics of the transfer function in (5), the tuning of the integral time constant $T_{i\omega}$ can be based on pole-zero cancellation by setting:

$$T_{i\omega} = \frac{T_a}{k_\omega} \tag{6}$$

This leads to a simplified expression of the open loop transfer function and the reduction of the degrees of freedom in the tuning to only the proportional gain. Indeed, the open loop transfer function is reduced to an integral term given as:

$$H_{OL\omega}(s) = \frac{k_{p\omega}}{T_a}\frac{1}{s} \tag{7}$$

The proportional gain $k_{p\omega}$ can then be selected to impose the cross over frequency $\omega_{c\omega}$ for the open loop transfer. This leads to:

$$\left|H_{OL\omega}(j\omega_{c\omega})\right| = \left|\frac{k_{p\omega}}{T_a}\frac{1}{j\omega_{c\omega}}\right| = 1 \tag{8}$$

$$k_{p\omega} = \omega_{c\omega}T_a \tag{9}$$

The Bode diagram of the open loop transfer function tuned according to the pole cancellation is shown in Fig. 5. For reference, the figure also includes the frequency characteristics obtained with two additional values for the integral time constant. These cases do not imply the order reduction of the transfer function due to the pole cancellation and are showing the impact higher or lower time-constants in the PI controller will have on the amplitude and frequency characteristics.

Assuming that T_a and k_ω of the VSM-based control is available to the synchronization controller, the closed loop transfer function can be then calculated as:

$$H_{CL\omega}(s) = \frac{H_{OL\omega}}{1+H_{OL\omega}} = \frac{1}{1+\frac{T_a}{k_{p\omega}}s} = \frac{1}{1+\frac{1}{\omega_{c\omega}}s} \tag{10}$$

The frequency characteristics of this transfer function are plotted in Fig. 6 for the reference configuration with a value of $\omega_{c\omega}$ equal to 2.5 rad/s, confirming the expected behaviour and bandwidth.

D. *Design of Outer Phase Difference Control Loop*

The phase angle alignment is ensured by the outer loop controller. Since the plant to be controlled includes the integration from frequency to phase angle as shown in Fig. 2, the open loop transfer function will contain a pure integrator. Thus, a Proportional (P) regulator will be sufficient for eliminating steady-state deviations in the phase angle. The outer loop open loop transfer function can be obtained from the closed loop transfer function (10) multiplied by the integration from the frequency to the phase angle, combined with a P regulator, and can be expressed as:

$$H_{OL\theta}(s) = k_{p\theta}H_{CL\omega}(s)\frac{2\pi\omega_b}{s} = k_{p\theta}\frac{2\pi\omega_b}{s}\frac{1}{1+\frac{1}{\omega_{c\omega}}s} \tag{11}$$

with $k_{p\theta}$ being the proportional gain of the controller. The model assumes the frequency to be expressed in per unit. Thus, the integration from per unit frequency to phase angle in rad/s requires scaling by the per unit angular frequency ω_b.

The closed loop transfer function can be then derived as:

$$H_{CL\theta}(s) = \frac{H_{OL\theta}(s)}{1+H_{OL\theta}(s)} = \frac{2\pi\omega_b k_{p\theta}\omega_{c\omega}}{s^2+\omega_{c\omega}s+2\pi\omega_b k_{p\theta}\omega_{c\omega}} \tag{12}$$

The tuning is intended to produce a smooth response without noticeable oscillations. Since the denominator of the closed loop transfer function is of second order, it can be convenient to rewrite it in a canonical form as

$$s^2 + 2\zeta\omega_n s + \omega_n^2 = 0\,. \tag{13}$$

Thus, the natural oscillation frequency ω_n and the damping ratio ζ, can be explicitly expressed by (14).

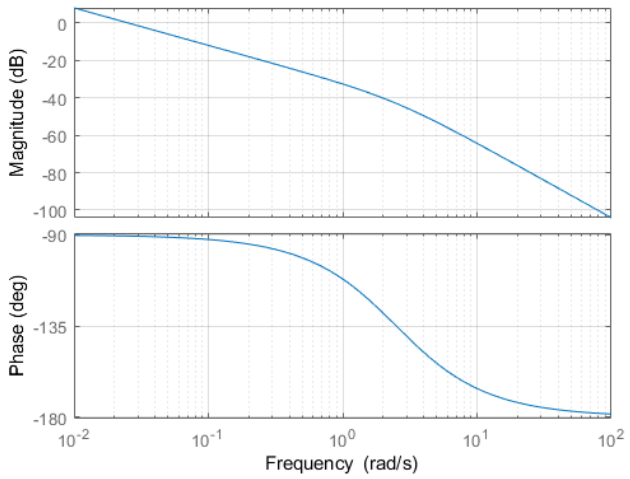

Fig. 7. Bode diagram of the open loop transfer function for phase controller

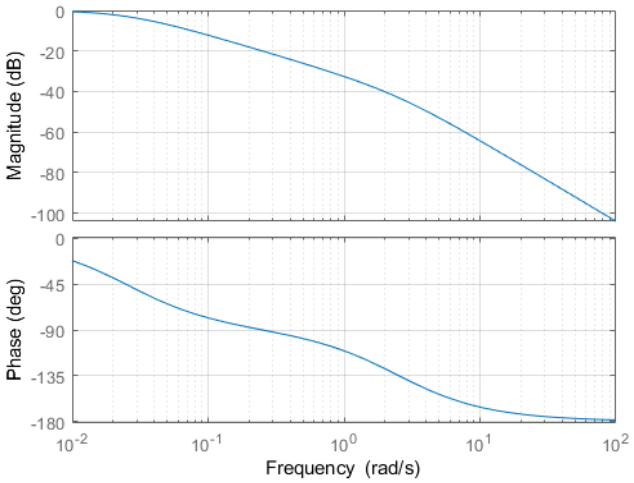

Fig. 8. Bode diagram of the closed loop transfer function for phase controller

$$\omega_n = \sqrt{2\pi\omega_b k_{p\theta}\omega_{c\omega}}$$
$$\zeta = \frac{\omega_{c\omega}}{2\sqrt{2\pi\omega_b k_{p\theta}\omega_{c\omega}}} = \sqrt{\frac{\omega_{c\omega}}{8\pi\omega_b k_{p\theta}}} \tag{14}$$

A convenient the tuning of the proportional gain $k_{p\theta}$ can then be obtained by imposing a specific damping ratio to achieve the desired characteristics of the time response

$$k_{p\theta} = \frac{\omega_{c\omega}}{8\pi\omega_b\zeta^2} \tag{15}$$

A suitable setting for the damping ratio can be $1/\sqrt{2}$, commonly referred to as optimal damping since this offers a balanced compromise between overshoot and settling time. This value for the damping ratio leads to. The resulting proportional gain can then be expressed as

$$k_{p\theta} = \frac{\omega_{c\omega}}{4\omega_b\pi} \tag{16}$$

The Bode diagrams for the open loop and closed loop transfer functions resulting from the tuning procedure defined by the results presented in this and previous subsection are shown in Fig. 7 and Fig. 8, respectively.

The substitution of the obtained expression for $k_{p\theta}$ in (16) into the open loop transfer function yields:

$$H_{OL\theta}(s) = \frac{\omega_{c\omega}}{2s}\frac{1}{1+\frac{1}{\omega_{c\omega}}s} = \frac{\omega_{c\omega}^2}{2s(\omega_{c\omega}+s)} \tag{17}$$

Thus, the crossover frequency for the outer loop can be then calculated as:

$$\omega_{c\theta} = \frac{\omega_{c\omega}}{\sqrt{2+2\sqrt{2}}} \tag{18}$$

This gives a reasonable upper limit for the crossover frequency of the phase angle control as a direct function of the crossover frequency selected for the inner loop frequency control.

IV. Simulation Results

The CCVSM scheme from Fig. 1 with the synchronization controller from Fig. 4 have been implemented in the Matlab Simulink environment and simulated for validating the grid resynchronization process in the time domain.

A. Effect of initial phase error on the resynchronization

As a first case the reference configuration with virtual inertia T_a = 2 has been simulated. The numerical simulation considers an initially islanded condition and covers the transient for the entire synchronization process including the closure of the breaker. The phase angle error and frequency error are displayed in Fig. 9 a). It is assumed that the synchronization has been completed when both these two errors are below a threshold value of 0.001. The direct and quadrature current components in the SRRF for the VSM, the grid and the load are displayed in Fig. 9b. The synchronization process is started at 2 s when the phase angle difference is about π rad. The islanded system operates at a lower frequency than the grid and this results in a constant error for the frequency and a continuously drifting phase error, appearing as a sawtooth signal with negative slope when resolved within ±π. Once the synchronization is activated, both the frequency and phase error are gradually reduced and converge to zero with almost negligible overshoot. The synchronization process is completed after about 3.5 s, as can be seen by the breaker being closed soon after t = 5.5 s. It can be noticed that the breaker operation initiates a transient on the currents. The transient in the load current is mainly caused by a small difference in the voltage amplitude when the breaker is closed. This could be avoided if an additional control loop was designed to regulate the voltage at the islanded side of the breaker to the same amplitude as at the grid side, for instance by acting on the voltage reference or the reactive power reference of the VSM. The reconnection to the grid also causes a small oscillation in the VSM current due to the inertial response of the change of load caused by the small change in voltage amplitude. This oscillation is also reflected in the grid currents, but is quickly damped according to the damping characteristics of the VSM

For completeness, the synchronization process has been repeated when starting from a phase angle error deviation close to −π, and the results are reported in Fig. 10. The response of the frequency and phase error appears with a different shape and the time required for resynchronization is slightly reduced. In general, the controller fulfilled in both cases the requirement for a smooth transient with negligible

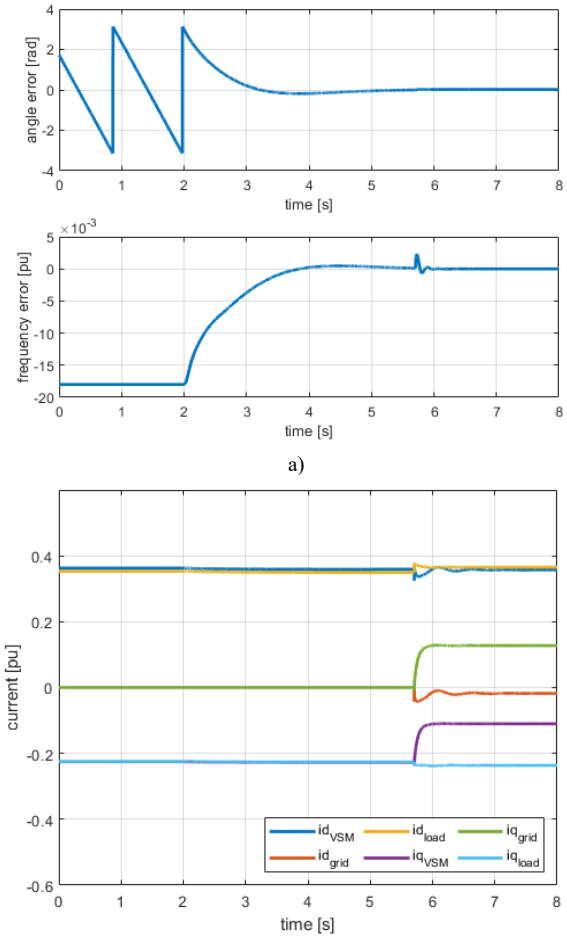

Fig. 9. Simulation results showing phase angle and frequency deviation during resynchronization for T_a =2 and positive initial phase error.

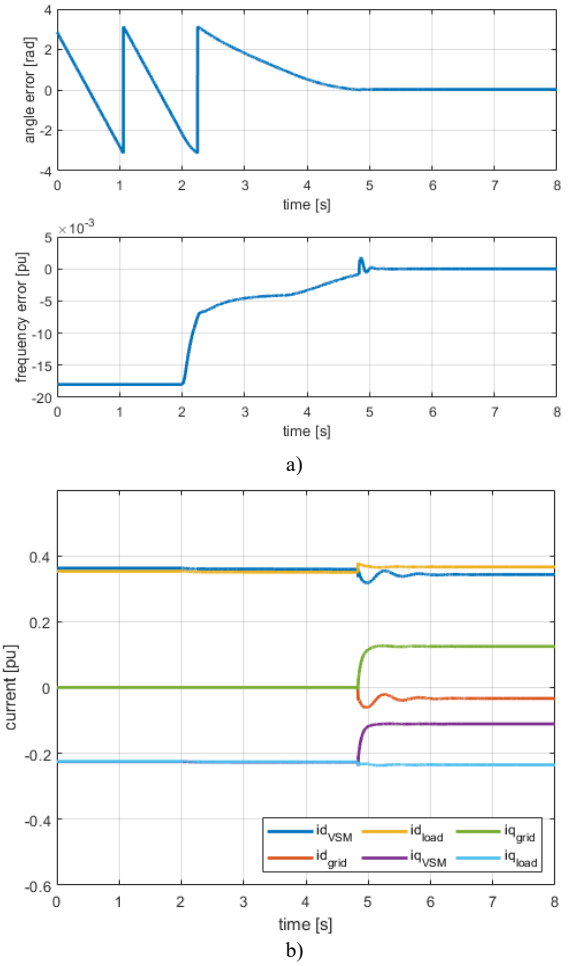

Fig. 10. Simulation results showing phase angle and frequency deviation during resynchronization for T_a =2 and negative initial phase error.

overshoot or oscillations. The synchronization controller has also been tested with positive values of the initial frequency error, resulting in qualitatively equivalent waveforms during the synchronization process.

B. Effect of inertia time constant on the resynchronization

The behaviour of the synchronization controller has been verified also for two other values of the inertia time constant T_a. In both cases the frequency controller has been retuned according to (6), (9) and (16) with $\omega_{c\omega}$ equal to 2.5 rad/s. However, due to the pole cancellation, differences in inertia time constant do not have an effect on the tuning of the proportional gain for the phase controller. In a first case the inertia time constant has been reduced to 0.5. The transient behaviour for the phase and frequency errors and for the currents is reported in Fig. 11. From a qualitative perspective this case presents very small differences compared to the previous examples. Moreover, these differences are mostly associated to the oscillations in the currents due to the reconnection. The transients for the frequency and phase errors are very close to the reference case as a consequence of the pole cancellation approach. In the second case the inertia time constant is increased to a value of 5 and results are displayed in Fig. 12. The results confirm again negligible differences in the transients of the phase and frequency errors. However, the differences in the currents after the reconnection are more noticeable. Indeed, this case results in more noticeable oscillations, which is mainly due to the higher virtual inertia.

V. Conclusion

Grid forming schemes, as the concept of Virtual Synchronous Machines (VSMs), offer the capability of providing smooth and seamless transition from grid connected mode to islanded mode. However, the inverse process requires a dedicated synchronization controller to ensure that the frequency and phase of the voltage in the islanded system are aligned with the grid voltage. This requires a controlled elimination of both phase and frequency deviations between the islanded system and the grid before reconnection. This paper presented a synchronization scheme based on a cascaded structure with an inner loop for synchronizing the frequency and an outer loop for aligning the phase. A tuning procedure for ensuring smooth and well damped transients of the resynchronization controller is also proposed. Both the scheme and the tuning procedure have been validated with numerical simulations. In particular, the simulation results indicate that the scheme performs satisfactorily and according to the expectations for a range of values of the inertia time constant and the initial phase error when the resynchronization process is started.

References

[1] H. Alrajhi Alsiraji, R. El-Shatshat, “Comprehensive assessment of virtual synchronous machine based voltage source converter controllers,” in IET Generation, Transmission, Distribution, vol. 11, no. 7, pp. 1762–1769, may 2017

[2] S. D'Arco, J. A. Suul, "Virtual Synchronous Machines – Classification of Implementations and Analysis of Equivalence to

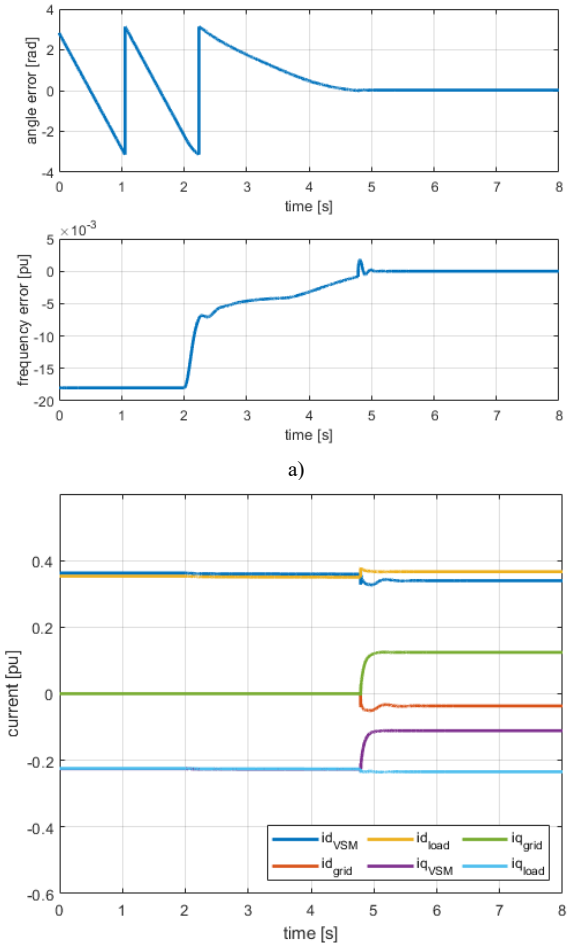

Fig. 11. Simulation results showing phase angle and frequency deviation during resynchronization for T_a = 0.5 and negative initial phase error.

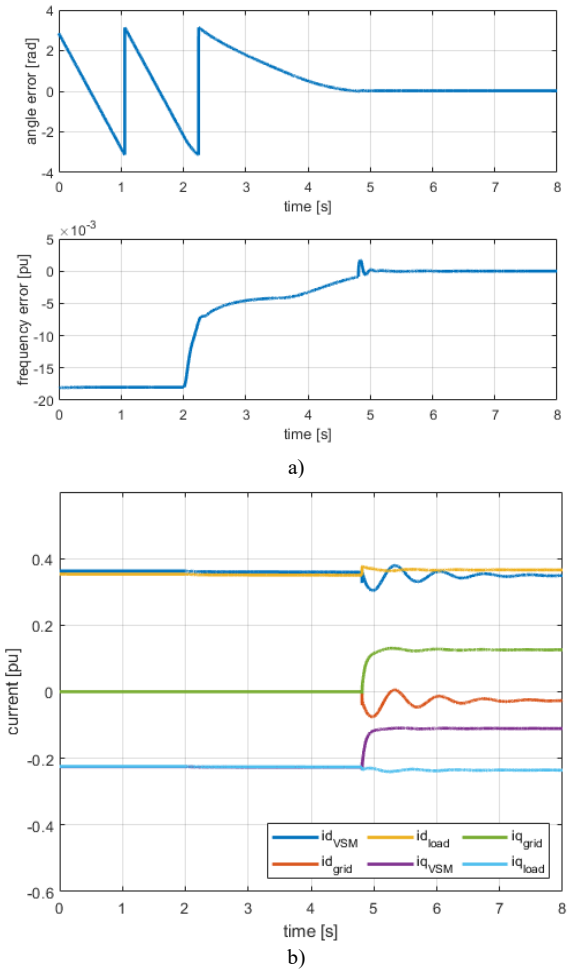

Fig. 12 Simulation results showing phase angle and frequency deviation during resynchronization for T_a = 5 and negative initial phase error.

Droop Controllers for Microgrids," in Proceedings of IEEE PES PowerTech 2013, Grenoble, France, 16-20 June 2013, 7 pp.

[3] H. Bevrani, T. Ise, Y. Miura, "Virtual synchronous generators: A survey and new perspectives," in *International Journal of Electric Power and Energy Systems*, vol. 54, pp. 244–254, January 2014

[4] M H. Othman, H. Mokhlis, M. Mubin, S. Talpur, N. F. Ab Aziz, M. Dradi, H. Mohamad, "Progress in control and coordination of energy storage system-based VSG: a review," in IET Renewable Power Generation, Vol. 14, No. 2, February 2020, pp. 177-187

[5] R. Hesse, D. Turschner, H.-P. Beck, "Micro grid stabilization using the Virtual Synchronous Machine (VISMA)," in *Proc. of the Int. Conf. on Renewable Energies and Power Quality*, ICREPQ'09, Valencia, Spain, 15-17 Apr. 2009, 6 pp.

[6] Y. Chen, R. Hesse, D. Turschner, H.-P. Beck, "Investigation of the Virtual Synchronous Machine in the Island Mode," in *Proc. of the 2012 3rd IEEE Innovative Smart Grid Technologies Europe Conf.*, ISGT Europe 2012, Berlin, Germany, 15-17 Oct. 2012, 6 pp.

[7] J. Rocabert, A. Luna, F. Blaabjerg, P. Rodríguez, "Control of Power Converters in AC Microgrids," in *IEEE Transactions on Power Electronics*, Vol. 27, No. 11, November 2012, pp. 4734-4749

[8] Y.-H. Yang, G.-C. Shang, Y-J. Fang, "A Fast Following Synchronizer of Generators," in *IEEE Transactions on Energy Conversion*, Vol. 3, No. 4, December 1988, pp. 765-769

[9] Y. Li, D. M. Vilathgamuwa, P. C. Loh, "Design, Analysis and Real-Time Testing of a Controller for Multibus Microgrid System," in *IEEE Transactions on Power Electronics*, Vol. 19, No. 5, September 2004, pp. 1195-1204

[10] C. Cho, J.-H. Jeon, J.-Y Kim, S. Kwon, K. Park, S. Kim, "Active Synchronizing Control of a Microgrid," in *IEEE Transactions on Power Electronics*, Vol. 26, No. 12, December 2011, pp. 3707-3719

[11] S. D'Arco, J. A. Suul, "A Synchronization Controller for Grid Reconnection of Islanded Virtual Synchronous Machines," in *Proceedings of the IEEE 6th International Symposium on Power Electronics for Distributed Generation*, PEDG 2015, Aachen, Germany, 22-25 June 2015, 8 pp.

[12] K.-Y. Choi, S.-I. Kim, S.-H. Jung, R.-Y. Kim, "Selective frequency synchronization technique for fast grid connection of islanded microgrid using prediction method," in *Int.Journal of Electrical Power & Energy Systems*, Vol. 111, October 2019, pp. 114-124

[13] J. Wu, F. Zhuo, Z. Wang, H. Yi, K. Yu, "Pre-synchronization method for grid-connection of virtual synchronous generators based micro-grids," in *Proceedings of the 2017 19th European Conference on Power Electronics and Applications,* EPE'17 ECCE Europe, Warsaw, Poland, 11-14 September 2017, pp. 1-8

[14] J. Wu, F. Zhuo, C. Zhu, Z. Wang, H. Yi, T. Wei, "Parameters Design of Pre-synchronization for Multiple Virtual Synchronous Generator Based Microgrid" *In Proceedings of the 2019 IEEE Applied Power Electronics Conference and Exposition*, APEC 2019, Anaheim, California, USA, 17-21 March 2019, pp. 3184-3188

[15] S. Chandak, P. Bhowmik, P. K. Rout, "Dual-stage cascaded control to resynchronise an isolated microgrid with the utility" in *IET Renewable Power Gene.*, Vol. 14, No. 5, April 2020, pp. 871-880

[16] S. Shah, H. Sun, D. Nikovski, J. Zhang, "VSC-Based Active Synchronizer for Generators," in *IEEE Transactions on Energy Conversion*, Vol. 33, No, 1, March 2018, pp. 116-125

[17] O. Mo, S. D'Arco, J. A. Suul, "Evaluation of Virtual Synchronous Machines with Dynamic or Quasi-stationary Machine Models," in *IEEE Trans. Ind. Electron.*, Vol. 64, No. 7, July 2017, pp. 5952-5962

[18] S. D'Arco, J. A. Suul, O. B. Fosso, "Small-Signal Modeling and Parametric Sensitivity of a Virtual Synchronous Machine," in *Proceedings of the 18th Power Systems Computation Conference*, PSCC 2014, Wrocław, Poland, 18-22 August 2014, 9 pp.

[19] S.-K. Chung, "A Phase Tracking System for Three Phase Utility Interface Inverters," in *IEEE Transactions on Power Electronics*, Vol. 15, No. 3, May 2000, pp. 431-438

[20] H. Kolstad, "*Control of an Adjustable Speed Hydro utilizing Field Programmable Devices*," Ph.D. Thesis, Norwegian University of Science and Technology, 2002